



CHORUS

This is the accepted manuscript made available via CHORUS. The article has been published as:

# High Resolution Transmission Electron Microscope Observation of Zero-Strain Deformation Twinning Mechanisms in Ag

L. Liu, J. Wang, S. K. Gong, and S. X. Mao

Phys. Rev. Lett. **106**, 175504 — Published 29 April 2011

DOI: [10.1103/PhysRevLett.106.175504](https://doi.org/10.1103/PhysRevLett.106.175504)

# A HRTEM Observation of Zero-strain Deformation Twinning Mechanisms in Ag

L. Liu<sup>1</sup>, J. Wang<sup>2\*</sup>, S. K. Gong<sup>1\*</sup>, S. X. Mao<sup>3\*</sup>

<sup>1</sup> School of Materials Science and Engineering, Beihang University, Beijing 100191, China

<sup>2</sup> MST-8, MS G755, Los Alamos National Laboratory, Los Alamos, NM 87545, USA

<sup>3</sup> Department of Mechanical Engineering and Materials Science, University of Pittsburgh, Pittsburgh, Pennsylvania 15261, USA

\*e-mail: [wangj6@lanl.gov](mailto:wangj6@lanl.gov); [gongsk@buaa.edu.cn](mailto:gongsk@buaa.edu.cn); [smao@enr.pitt.edu](mailto:smao@enr.pitt.edu)

## ABSTRACT

We have observed a new deformation twinning mechanism using HRTEM in polycrystalline Ag films, zero strain twinning via the nucleation and migration of  $\Sigma 3\{112\}$  incoherent twin boundary (ITB). This twinning mechanism produces a near zero macroscopic strain because the net Burgers vectors either equals to zero or is equivalent to a Shockley partial dislocation. This observation provides new insight in understanding deformation twinning and confirms a previous hypothesis: **de-twinning** could be accomplished via the nucleation and migration of  $\Sigma 3\{112\}$  ITBs. The zero-strain twinning mechanism may be unique to low stacking fault energy metals with implications for their deformation behavior.

**Key Words:** deformation twinning; rolling; Ag; TEM

Twinning is a typical plastic deformation mechanism, accomplished by the glide of twinning dislocations (TDs) to generate macroscopic strain [1, 2]. Deformation twinning has been widely observed in materials with different crystal structures, such as body-centered-cubic (bcc) [1], face-centered-cubic (fcc) [3-8], hexagonal-close-packed (hcp) [9-13], and others [14-16]. For fcc metals, the tendency of deformation twinning is mainly determined by its stacking fault energy (SFE) [17]. For fcc metals with medium-to-high SFEs such as Cu and Al, dislocation slip is the preferred plastic deformation mechanism for coarse-grained metals. For fcc metals with low SFE like Ag, plastic deformation is accomplished by a combination of dislocation slip and deformation twinning [18]. Many twinning mechanisms have been proposed, including the pole mechanisms [19], prismatic glide [20], faulted dipole [16], and others [14,15]. These deformation twins are accomplished by the glide of twinning dislocations (TDs). TDs usually all have the same Burgers vector so that the Peach-Koehler glide forces on the TDs have the same sign and they move along the same direction [2]. As a consequence of twin propagation, a net macroscopic strain is generated.

Is it true that deformation twinning always produces a net macroscopic strain? Recently, Wu *et al.* proposed a new twinning mechanism, random activation of partials (RAP), to explain the zero net macroscopic strain phenomena associated with twinning in nanocrystalline Al, Ni, and Cu [21]. It is noticed that since the participating Burgers vectors sum to zero in the random activation of partials mechanism, RAP twinning must produce zero net macroscopic strain. More recently, Wang *et al.* reported their in-situ TEM observation and revealed a new de-twinning mechanism in Cu, in which de-twinning is accomplished via the collective glide of  $\Sigma 3\{112\}$  ITBs [22-25]. Since  $\Sigma 3\{112\}$

ITBs can be presented with a set of Shockley partial dislocations with a repeatable sequence  $b_2:b_1:b_3$  on every (111) plane [22], a noteworthy characteristic of the three partial dislocations is that the sum of their Burgers vectors in one unit equals zero [22, 23]. Accompanying with de-twinning in Cu, the net macroscopic strain must be zero. Some analogous mechanisms had been postulated by Christian who **explained** the fcc to hcp transformation in metals [26] and by Mahajan *et al.* [27] to explain the formation for annealing twins.

It is still a puzzle why such twin boundaries (front tip of deformation twins) move under zero or very small net Peach-Koehler force due to the zero net Burgers vectors. It was understood that the transformation [26] and annealing twinning [27] can be driven by the Gibbs free energy difference, and the de-twinning mechanisms for thin twin **lamellae** can be driven by reducing the area of twin boundaries [25]. Comparing with the above mechanisms [25-27], deformation twinning through the mechanisms in Refs. [21, 25] will create new high-energy twin boundaries, thus it is not energetically favorable. To explain the motion of such boundaries, Wu *et al.* [21] proposed the RAP mechanisms, i.e, the random nucleation and emission of partials at GBs in nanocrystalline **metals**. It is possible for small grain size due to the stress fluctuation. However, the nucleation could be random for partials with different Burgers vectors due to the local stresses, but the further gliding of partials must be subjected to a positive Peach-Koehler force [2]. Thus, Wang *et al.* propose a stop/start, move/drag, partial dislocation mechanism [25], in which  $\Sigma\{112\}$  ITB **goes** from an equilibrium state, to a non-equilibrium state, then back to an equilibrium state again. **They also observed that ITBs could be pinned due to the interaction of lattice dislocation with ITBs using in situ TEM [24].** But the experiment

evidence is still insufficient corresponding to deformation twinning via the collective glide of ITBs.

In this letter, we report deformation-twinning mechanisms, with a focus on the zero strain deformation twinning, in polycrystalline Ag films. Owing to the low SFE, deformation twinning in Ag is easily activated. The further analysis is performed at a high resolution transmission electron microscope (HRTEM) to identify twins and twinning mechanisms combining with dislocation theory and atomistic simulations.

High purity 99.99% silver films with the thickness of 1 mm were used for the experiment. Annealing was carried out at 1073K, less than  $10^{-4}$  Pa to eliminate crystalline defects. After annealing, the films were cooled in liquid nitrogen, and then immediately rolled to 50  $\mu\text{m}$  thickness (95% rolling strain) at room temperature. The 3-mm diameter transmission electron microscope (TEM) specimen were cut from the films, and thinned by double-jet electro polishing in solution of 10% perchloric acid, 10% glycerol and 80% methanol at 213K in a TenuPol-5 electropolisher. TEM observation was conducted using a JEM2100F microscope with a point-to-point resolution of 0.23 nm.

Fig. 1 (a) is taken after annealing, showing no twins while dislocation lines can be observed, although minor annealing twins have been found elsewhere. After mechanical rolling, Fig. 1(b) and (c) show a lot of twins observed in grains (the grain size  $\sim 1 \mu\text{m}$ ). These twins have an average thickness of 50~60 nm and two types of twin boundaries,  $\Sigma\{111\}$  coherent twin boundaries (CTBs) and  $\Sigma\{112\}$  incoherent twin boundaries (ITBs). For most twins, one of two ends is at grain boundary and the other end is inside of grains. Dislocation debris has been found in other area under HRTEM although Fig. 1(c) shows dislocation free with the regular TEM image. Two regions in Fig. 1(c) are

marked for the further analysis. It is worth mentioning that the region R2 shows a twin with both ends inside of the grain.

To identify the **characteristics** of the front tips of deformation twins, HRTEM analysis **is** conducted for regions R1 and R2 (Fig. 1c). It is noted that (1) a repeated pattern with the periodicity of three times of the interplanar spacing of  $\{111\}$  planes is clearly observed (**Fig. 2(b), (c) and (e)**), (2) the 9R structure is bounded between the two phase boundaries<sup>1</sup>, PB1 and PB2 (Figs. 2(b) and (e)), and (3) the extra spots **compared** to regular fcc  $\langle 110 \rangle$  SAED (**Fig. 2(f)**). All these **points** confirm that the ends of twins are  $\Sigma 3\{112\}$  ITBs. In addition, the most intriguing result from the TEM analysis of R2 is that the twin has  $\Sigma 3\{112\}$  ITBs as both ends, which supports our hypothesis that deformation twins can propagate with the front end as  $\Sigma 3\{112\}$  ITBs, i.e., the sum of Burgers vectors of partials at the front is equal to zero.

However, it is not clear whether these twins are experiencing twinning processes or de-twinning processes. Fig. 3 shows a series of TEM images containing a twin end —  **$\Sigma 3\{112\}$  ITB**. The width of the 9R structure is initially measured about 12.5 nm, then reduces to 4.5 nm and finally is stabilized at 1.2 nm, which is close to the equilibrium distance of 1.0 nm at zero applied shear stress [23]. It is worth mentioning that (1) PB1 moves downwards, (2) PB2 moves upwards, but (3) PB2 moves slower than PB1. This collapse process can be ascribed to the relaxation of the pre-existing internal stresses by electron beam annealing applied in the TEM sample. Accompanying with the relaxation of internal stresses, the initial equilibrium on the force applied to partials can be

---

<sup>1</sup> PB1 represents an array of Shockley partial dislocations  $b_1$  separated by every two  $\{111\}$  atomic planes **acting** as the front tip of the deformation twins; PB2 represents an array of Shockley partial dislocations **separated by every  $\{111\}$  atomic plane with a consequence  $b_2:b_3$**  in the boundary of the twin and 9R structure.

destroyed, resulting in the glide of both boundaries corresponding to the reduction of the width of the 9R structure. The moving distances for PB1 about 10 nm downwards and for PB2 1.0 nm upwards. The difference of the moving distances implies that PB2 experiences a higher Peierls force than PB1. To address the influence of the local shear stress on the atomic structures of  $\Sigma 3\{112\}$  ITBs, we conducted molecular dynamics simulations for Ag. As shown in Fig 3(d), owing to the mirror symmetry of two crystals across a twin boundary, Shockley partial dislocations  $b_1$  (forming PB1) could be in the left or the right side of the boundary PB2 at zero applied shear stress. At a certain applied shear stress, Shockley partial dislocations  $b_1$  only can be in one side corresponding to the Peach-Koehler force, for example of the lower configuration in Fig. 3(d) with shear stress of 100 MPa. In other words, the position of PB1 at the applied shear stresses serves as a flag, indicating the propagation of a twin along the twinning direction (twinning when the PB1 acts as the boundary between the matrix and the 9R structure) or along the opposite direction (de-twinning when the PB1 acts as the boundary between the twin and the 9R structure). Combining in-situ TEM results with atomistic simulations, we can find that (1) the internal stresses exist in the rolled Ag films in Figs 2 or 3(a), and (2) the net Peach-Koehler force acting on the Shockley partials  $b_1$  (PB1) towards the twinning direction of the deformation twin because of the PB1 acting as the boundary between the matrix and the 9R structure, implying that *the deformation twins observed in Ag is experiencing a twinning process.*

Coupling atomistic simulations and experimental observations, we here discuss the motion mechanism of ITBs. When the ITB is subjected to a shear stress  $\tau$ , the Peach-Koehler glide force on the partial dislocation  $b_1$  is composed of the contribution of the

applied shear stress, the contributions of dislocation interactions, the interface tension arising from the stacking fault, and any Peierls force or other friction type force. The Peierls force may be negligible for  $b_1$ , typical of isolated partials in fcc metals [2]. However, a Peierls force may be present for the paired partials  $b_2$  and  $b_3$  (illustrated in Fig 3(d)), as implied by in-situ TEM observation (Fig. 3), because they remain closely spaced in the residual ITB and may correspond to a relaxed nonlinear structure (the paired partials are hard to **break away** from each other due to the attractive force originating from the interaction of their screw components). When the ITB (containing three types of dislocations), whether compact or dissociated, is in the equilibrium state, the net force equals to zero regardless of the magnitude of the applied shear stresses. For the near equilibrium state, a slight increase in stress would move the partial dislocation  $b_1$ , because the partial dislocation  $b_1$  is initially more mobile than the other two partial dislocations [22]. For the first scenario an increased stress is required for the partial dislocation  $b_1$  to overcome the interaction force, but the latter drops as it moves tending to produce breakaway at constant stress. However, locally the plastic strain associated with the motion of the partials should produce a load drop, tending to arrest the motion of partial  $b_1$ . The load drop would be permanent under constant applied strain, or temporary (over a period where an elastic wave reaches the remote free surface and returns) under constant applied load. Then the paired partials ( $b_2$  and  $b_3$ ) would have SFE plus the interaction force pulling them and decreased applied force acting on the paired partials so they could move to approach the  $b_1$  partial until again reaching the equilibrium spacing. This process could repeat, resulting in the migration of ITBs in the direction favored by the applied force acting on the  $b_1$  partials, during which zero deformation twin



is developed. Locally, the situation would represent a stop/start, jump/drag displacement situation with some waiting time [25].

It is worth to discuss the nucleation of such zero-strain deformation twins. As observed in TEM images, most deformation twins originate at grain boundaries. Similar to a grain boundary nucleation mechanism in nanocrystalline materials [21] and a dissociation mechanism of grain boundary dislocations in Mg [28, 29], the nucleation of a deformation twin with  $\Sigma 3\{112\}$  ITBs as its front tip may require some structural characteristics of the grain boundary, for example, the grain boundary is close to  $\Sigma 3\{112\}$  ITBs, then dissociate to one  $\Sigma 3\{112\}$  ITB and the other grain boundary. Further TEM studies are required to address the structural characteristics of grain boundaries.

In a summary, we have observed a new deformation twinning mechanism using HRTEM in polycrystalline Ag films, twinning via the migration of  $\Sigma 3\{112\}$  ITBs. As a result of the net zero Burgers vector at the twin front, this twinning mechanism does not produce macroscopic strain. This observation provides an evidence for our previous hypothesis (de-twinning could be accomplished via the nucleation and migration of  $\Sigma 3\{112\}$  incoherent twin boundary at grain boundaries) [25], and opens a new insight in understanding deformation twinning, especially the effect of atomic structures of grain boundaries [28, 29].

### **Acknowledgements**

SG acknowledges the support from NSFC No. 50731001. JW acknowledges the support provided by the *Center for Materials at Irradiation and Mechanical Extremes*, an Energy Frontier Research Center funded by the U.S. Department of Energy, Office of Science, Office of Basic Energy Sciences under Award Number **2008LANL1026**, and also acknowledge support provided by the Los Alamos National Laboratory Directed Research and Development (LDRD). S.M. would like to acknowledge NSF CMMI 08 010934 through University of Pittsburgh.

## References

- [1] J.W. Christian and S. Mahajan, *Prog. Mater. Sci.* **39**, 1 (1995).
- [2] J. P. Hirth and J. Lothe, *Theory of Dislocations* (Krieger, Melbourne, FL, 1992).
- [3] V. Yamakov, D. Wolf, S. R. Phillpot, and H. Gleiter, *Acta Mater.* **50**, 5005 (2002).
- [4] Z. W. Shan, L. Lu, A. M. Minor, E. A. Stach, and S. X. Mao, *JOM* **60(09)**, 71 (2008).
- [5] E. Ma, Y. M. Wang, Q. H. Lu, M. L. Sui, L. Lu, and K. Lu, *Appl. Phys. Lett.* **85**, 4932 (2004).
- [6] J. Wang and H. Huang, *Appl. Phys. Lett.* **88**, 203112 (2006).
- [7] M. W. Chen, E. Ma, K. J. Hemker, H. W. Sheng, Y. M. Wang, and X. M. Cheng, *Science* **300**, 1275 (2003).
- [8] X. Z. Liao, Y. H. Zhao, S. G. Srinivasan, Y. T. Zhu, R. Z. Valiev, and D. Gunderov, *Appl. Phys. Lett.* **84**, 592 (2004).
- [9] L. Wang, P. Eisenlohr, Y. Yang, T. R. Bieler, and M. A. Crimp, *Scripta Mater.* **63**, 827 (2010).
- [10] L. Wang, Y. Yang, P. Eisenlohr, T. R. Bieler, M. A. Crimp, and D. E. Mason, *Metall. Mater. Trans. A* **41**, 421 (2010).
- [11] C. N. Tomé and G. C. Kaschner, *Mater. Sci. Forum* **495-497**, 1001 (2005).
- [12] J. Wang, J. P. Hirth, and C. N. Tomé, *Acta Mater.* **57**, 5521 (2009).
- [13] J. Wang, R. G. Hoagland, J. P. Hirth, L. Capolungo, I. J. Beyerlein, and C. N. Tomé, *Scripta Mater.* **61**, 903 (2009).
- [14] S. Mahajan and G. Y. Chin, *Acta Metall.* **21**, 1353 (1973).
- [15] N. Thompson, *Proc. Phys. Soc. B* **66**, 481 (1953).
- [16] M. Niewczas and G. Saada, *Philos. Mag. A* **82**, 167 (2002).
- [17] H. Van Swygenhoven, P. M. Derlet, and A. G. Frøseth, *Nat. Mater.* **3**, 399 (2004).
- [18] E. B. Tadmor and N. Bernstein, *J. Mech. Phys. Solids.* **52**, 2507 (2004).
- [19] A. Ookawa, *J. Phys. Soc. Jpn.* **12**, 825 (1957).
- [20] J. A. Venables, *Philos. Mag. A* **6**, 379 (1961).
- [21] X. L. Wu, X. Z. Liao, S. G. Srinivasan, F. Zhou, E. J. Lavernia, R. Z. Valiev, and

- Y. T. Zhu, Phys. Rev. Lett. **100**, 095701 (2008).
- [22] J. Wang, O. Anderoglu, J. P. Hirth, A. Misra, and X. Zhang, Appl. Phys. Lett. **95**, 021908 (2009).
- [23] J. Wang, A. Misra, and J. P. Hirth, Phys. Rev. B (2011) DOI: 10.1103/PhysRevB.00.004100.
- [24] N. Li, J. Wang, J. Y. Huang, A. Misra, and X. Zhang, Scripta Mater. **64**, 149 (2011).
- [25] J. Wang, N. Li, O. Anderoglu, X. Zhang, A. Misra, J. Y. Huang, and J. P. Hirth, Acta Mater. **58**, 2262 (2010).
- [26] J. W. Christian, *The Theory of Transformations in Metals and Alloys* (Pergamon, New York, 1965).
- [27] S. Mahajan, C. S. Pande, M. A. Imam, and B. B. Rath, Acta Mater. **45**, 2633 (1997).
- [28] J. Wang, I. J. Beyerlein, and C. N. Tomé, Scripta Mater. **63**, 741 (2010).
- [29] I. J. Beyerlein and C. N. Tomé, Proc. R. Soc. A **466**, 2517 (2010).

### Captions of Figures:

Figure 1. (a) TEM image of the silver after annealing. (b) and (c) TEM images of the silvers at grain size ( $\sim 1\mu\text{m}$ ) after cold **rolling** to 95% strain, showing twins with the average twin thickness of 50~60 nm, and two types of twin boundaries: coherent twin boundaries (CTBs) and incoherent twin boundaries (ITBs). For most twins, one of two ends is at grain boundary and the other end is inside of grains. Two regions, R1 and R2 in (c) are marked for the further analysis.

Figure 2. Characterization of the front end of deformation twins. (a), (b) and (c) correspond to region 1 in Fig. 1 (c): (a) the magnification of R1, (b) HRTEM image of the front end composed of PB1, 9R, and PB2, and (c) the magnification of PB1 shows Shockley partial dislocations separated by every three atom planes. (d) and (e) correspond to region 2 in Fig. 1(c): (d) the magnification of R2, and (e) HRTEM image of one end of the deformation twin, showing a wider **ITB** composed of PB1, 9R, and PB2. In (b) and (e), PB1 represents an array of Shockley partial dislocations  $b_1$  separated by every two  $\{111\}$  atomic planes act as the front tip of the deformation twins; PB2 represents an array of Shockley partial dislocations **separated by every one  $\{111\}$  atomic plane with a consequence  $b_2:b_3$**  in the boundary of the twin and 9R structure. (f)  $\langle 110 \rangle$  SAED pattern corresponding to (e) shows the extra spots in comparison with a normal fcc structure. The symbol “ $\perp$ ” indicates Shockley partial dislocations  $b_1$  in the PB1.

Figure 3. A series of snapshots showing the collapse of 9R structure during TEM observation, from (a) initial 12.5 nm, to (b) 4.0 nm, to (c) a stable size of 1.2 nm. The collapse of 9R structure is accomplished via the glide of PB1 and PB2. PB1 moves 10 nm downwards and PB2 moves 1.0 nm upwards from (a) to (c). (d) Atomic structures of  $\Sigma 3\{112\}$  ITBs in Ag. The top shows the equilibrium structure at zero applied shear stress and the lower at the applied shear stress of 100 MPa.

Figure 1

Liu *et al.*

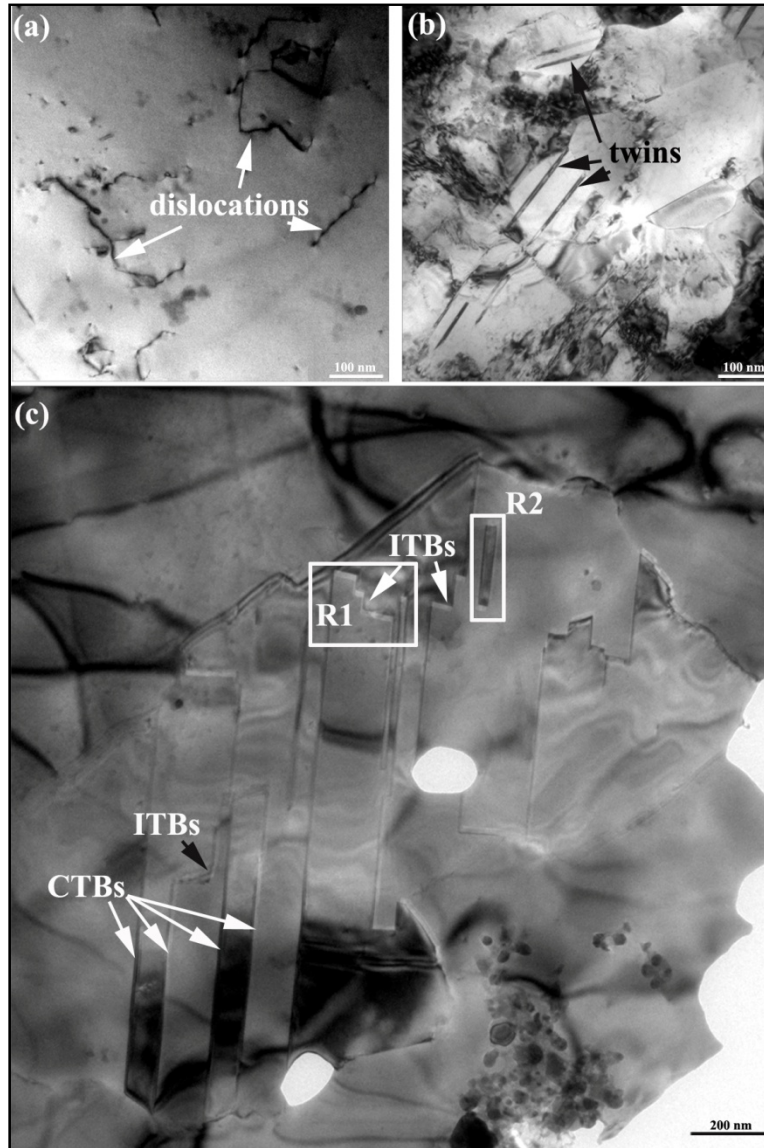


Figure 2

Liu *et al.*

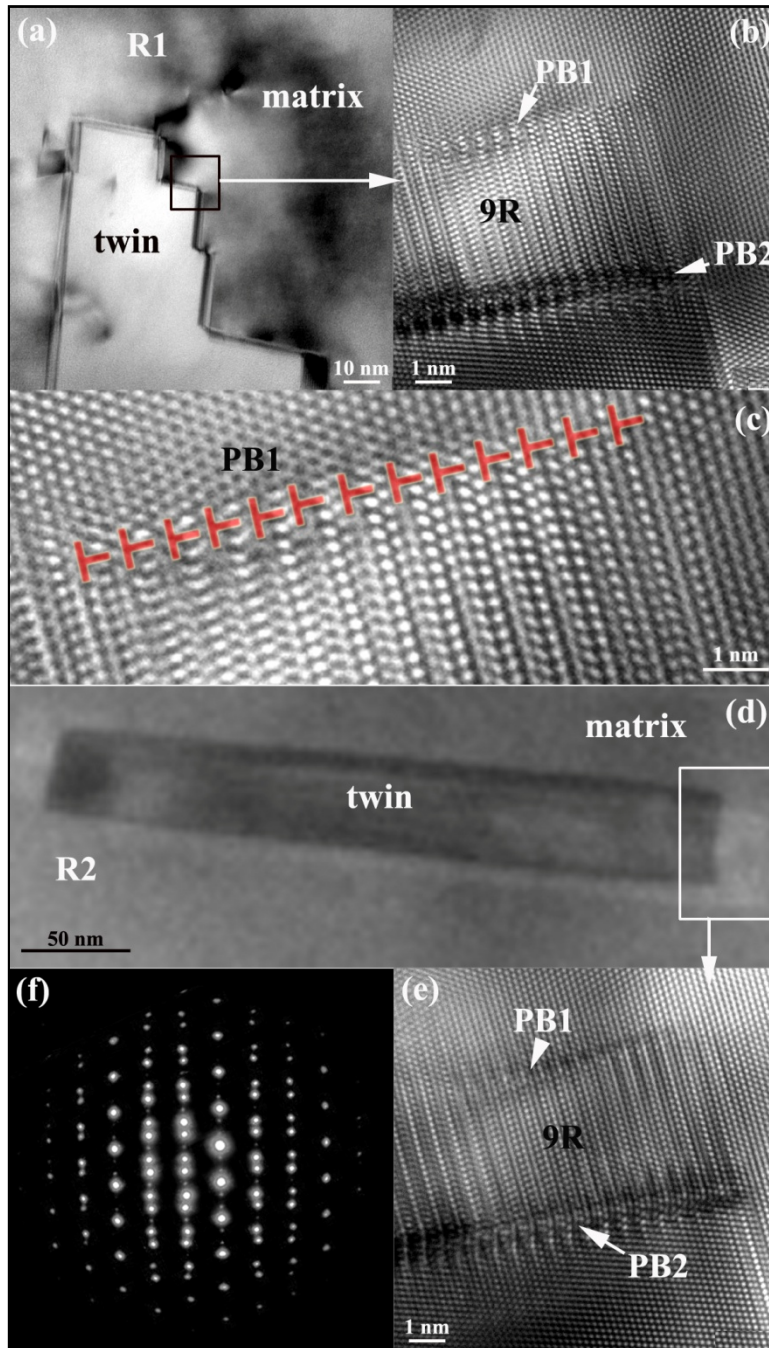


Figure 3

Liu *et al.*

